Hierarchical glycolytic pathways control the carbohydrate utilization regulator in human gut *Bacteroides*

Seth G. Kabonick[a,b,c], Kamalesh Verma[a,b,c], Jennifer L. Modesto[a,b,c], Victoria H. Pearce[a,b,c], Kailyn M. Winokur [a,b,c], Eduardo A. Groisman[d], and Guy E. Townsend 2nd,[a,b,c]

[a]*Penn State College of Medicine, Hershey, PA, USA*

[b]*Penn State One Health Microbiome Center, Pennsylvania State University, State College, PA, USA*

[c]*Center for Molecular Carcinogenesis and Toxicology, Pennsylvania State University, State College, PA, USA*

[d]*Yale University School of Medicine, New Haven, CT, USA*

*Address correspondence to Guy E. Townsend: gtownsend@pennstatehealth.psu.edu; Department of Molecular and Precision Medicine, Penn State College of Medicine, 700 HMC Crescent Road, Hershey, Pennsylvania, USA

Abstract

Human dietary choices control the gut microbiome. Industrialized populations consume abundant amounts of glucose and fructose, resulting in microbe-dependent intestinal disorders. Simple sugars inhibit the carbohydrate utilization regulator (Cur), a transcription factor in members of the prominent gut bacterial phylum, *Bacteroidetes*. Cur controls products necessary for carbohydrate utilization, host immunomodulation, and intestinal colonization. Here, we demonstrate how simple sugars decrease Cur activity in the mammalian gut. Our findings in two *Bacteroides* species show that ATP-dependent fructose-1,6-bisphosphate (FBP) synthesis is necessary for glucose or fructose to inhibit Cur, but dispensable for growth because of an essential pyrophosphate (PPi)-dependent enzyme. Furthermore, we show that ATP-dependent FBP synthesis is required to regulate Cur in the gut but does not contribute to fitness when *cur* is absent, indicating PPi is sufficient to drive glycolysis in these bacteria. Our findings reveal how sugar-rich diets inhibit Cur, thereby disrupting *Bacteroides* fitness and diminishing products that are beneficial to the host.

Introduction

Humans can consume over 3 times the recommended amounts of glucose and fructose, monosaccharides abundant in ultra-processed foods and beverages containing high fructose corn syrup[1]. Overconsumption of these sugars supersedes the absorptive capacity of the small intestine to reach the distal gut, where they are consumed by resident microbes[2]. High-sugar diets alter gut microbial composition and gene transcription, thereby increasing microbiota-dependent disease susceptibility[3,4]; however, the microbial processes that mediate sugar-rich, diet-dependent changes in the gut are not understood. Therefore, it is necessary to investigate the mechanisms by which refined sugar consumption reduces commensal fitness and disrupts beneficial microbiota-host interactions.

Carbon catabolite repression (CCR) is a global regulatory mechanism that prioritizes the utilization of preferred carbon sources over other available substrates[5-7]. In *Escherichia coli* (*Ec*), glucose and fructose impose CCR effects via the phosphoenolpyruvate (PEP):carbohydrate phosphotransferase system (PTS), which utilizes PEP to concomitantly import and phosphorylate target monosaccharides[8,9]. *Ec* employs the PTS to couple intracellular metabolite pools with sugar internalization and entry into central metabolism[10-12]. Ultimately, substrate phosphorylation by the PTS reduces cyclic adenosine monophosphate (cAMP) production, the allosteric activator of cAMP Receptor Protein (CRP), thereby reducing the expression of CRP-dependent genes, which mediate the utilization of less-preferred carbon sources[8,13]. Similar to CRP in *Ec*, *Bacteroides* encodes Cur, a transcription factor that is required for growth on several carbohydrates[14-16]; however, *Bacteroides* species lack both endogenous cAMP and PTS orthologs, indicating that a distinct CCR-like mechanism controls Cur activity[17-19]. Moreover, *Bacteroides* recognizes carbohydrates and initiates transcription in the periplasm before entering central metabolism[14-16], further obscuring how sugars reduce Cur activity.

Cur regulates over 400 genes in the model organism, *Bacteroides thetaiotaomicron (Bt)*[12], including products necessary for glycan utilization[20], intestinal colonization[10,21], and beneficial host interactions[4]. For example, *cur* is required for the expression of *fucI-fucR,* an operon that is necessary for fucose utilization[10,11]. Fucose is a constituent monosaccharide that decorates host mucosal glycans mediating a trans-kingdom signaling axis in the gut[22]. In addition, the *cur*-dependent gene, *fusA2*, encodes an alternative translation elongation factor that facilitates GTP-independent protein synthesis, a process necessary for intra-intestinal fitness[23]. Cur is also responsible for the expression of many polysaccharide utilization loci (PUL) that are important for providing *Bt* access to host- and dietary-derived nutrients. For example, PUL80 expression requires *cur* and contains *BT4295,* a putative chitobiase (chb^{PUL80}) that directs immunotolerogenic

62 T-cell development to reduce host-disease susceptibility[4]. Accordingly, a simple sugar diet
63 reduces *chb*^{PUL80} expression by inhibiting Cur activity, thereby disrupting T-cell differentiation and
64 initiating colitis in mice[4]. Therefore, it is necessary to understand how simple sugars inhibit Cur
65 activity for both bacterial fitness and host physiology.
66 Here, we report that Cur inhibition by glucose and fructose requires corresponding ATP-
67 dependent hexokinases that facilitate their utilization. We establish that simple sugars impose
68 CCR-like effects via a unique mechanism in *Bacteroides*, whereby phosphorylated sugars are
69 converted into the ubiquitous metabolite – fructose-1,6-bisphosphate (FBP) – by distinct ATP- and
70 PPi-dependent enzymes. Strikingly, ATP-dependent FBP synthesis is required for Cur inhibition
71 by dietary sugars and necessary for *in vivo* fitness when *cur* is present, but otherwise dispensable
72 for cell growth. In contrast, PPi-dependent FBP synthesis is essential for growth, indicating that
73 PPi, rather than ATP, drives glycolysis in these organisms. Our findings identify unique pathways
74 in *Bacteroides* that coordinate CCR-like effects on Cur activity in the presence of dietary sugars,
75 thereby silencing colonization factor expression, hindering intra-intestinal fitness, and reducing
76 products beneficial to host health.
77
78 **Results**
79 **Glucose and fructose inhibit Cur activity in a dominant, dose-dependent manner.**
80 We previously demonstrated that *fusA2* is the most highly upregulated *cur*-dependent
81 gene identified to date and Cur binding to the *fusA2* promoter region is necessary for *Bt* fitness in
82 the murine gut[12]. To kinetically examine Cur activity during growth, we generated P-*fusA2* by
83 introducing the *fusA2* promoter into *pBolux*, a reporter plasmid containing a *Bacteroides*-
84 optimized luciferase cassette[24]. A *wild-type Bt* strain harboring P-*fusA2* exhibited higher
85 bioluminescence than an isogenic strain harboring the promoter-less *pBolux* control plasmid in
86 the *cur*-dependent substrates fucose (Fig. 1a) and N-acetylgalactosamine (galNAc) (Fig. 1b)[25]. In
87 contrast, this strain exhibited decreasing bioluminescence during growth on the *cur*-independent
88 monosaccharides, fructose or glucose (Fig. 1c & Extended Data Fig. 1a). When cultured in
89 porcine mucosal O-glycans (PMOG), a mixture that increases *cur*-dependent gene
90 transcription[10,20], the *wild-type* strain harboring P-*fusA2* produced a 45-fold increase in
91 bioluminescence by 18 hours (Fig. 1d). Bioluminescence from P-*fusA2* requires Cur activity
92 because a *wild-type Bt* strain harboring P-*fusA2* but lacking the 22 base pair Cur binding site[12]
93 (P-*Δ22bp*) exhibited indistinguishable bioluminescence relative to strains harboring *pBolux* (Fig.
94 1a, b, c & Extended Data Fig. 1a, b, c). Similarly, a *cur*-deficient strain (*Δcur*) harboring P-*fusA2*
95 produced bioluminescence comparable to *pBolux* when grown in identical conditions (Fig. 1c &

96 Extended Data Fig. 1a, d, e). Bioluminescence from the *wild-type* strain harboring P-*fusA2*
97 supplied PMOG and monosaccharide mixtures were altered according to the sugar identity. For
98 example, mixtures containing galNAc initially reduced, but ultimately increased bioluminescence,
99 whereas mixtures containing fucose initially had no effect but eventually increased
100 bioluminescence above cells grown in PMOG alone (Extended Data Fig. 1f). Alternatively, a *wild-*
101 *type* strain harboring P-*fusA2* supplied PMOG with increasing concentrations of fructose or
102 glucose elicited corresponding reductions in bioluminescence (Fig. 1d & Extended Data Fig. 1g),
103 similar to previously reported *cur*-dependent transcript levels[10]. Bioluminescence specifically
104 reports changes in Cur activity because neither *Δcur* harboring P-*fusA2* nor the *wild-type* strain
105 harboring P-*Δ22bp* produced increases compared to isogenic strains harboring p*Bolux* in all
106 examined conditions (Extended Data Fig. 1b, c, d, e). Bioluminescence did not reduce cellular
107 growth because strains harboring P-*fusA2* or P-*Δ22bp* grew comparably to isogenic strains
108 harboring p*Bolux* in *cur*-dependent or -independent conditions (Extended Data Fig. 1h, i).
109 Importantly, *cur* is dispensable for reporter functionality because a strain harboring P-*PUL22*[24], a
110 reporter containing the promoter region of the fructan utilization PUL (Extended Data Fig. 2a),
111 exhibited bioluminescence resembling a *wild-type Bt* strain (Extended Data Fig. 2b) when cultured
112 in PMOG supplemented with fructose, although slightly delayed due to a growth defect (Extended
113 Data Fig. 2c). Collectively, these data establish that glucose and fructose inhibit Cur activity in a
114 dominant and dose-dependent manner and that P-*fusA2* faithfully reports previously observed
115 *cur*-dependent transcript levels[10].
116
117 **Cur inhibition by fructose and glucose requires ATP-dependent substrate**
118 **phosphorylation.**
119 Many other bacterial taxa alter transcription following sugar transport into the cytoplasm[26];
120 however, *Bacteroides* senses sugars prior to transport[14,24], complicating the way fructose or
121 glucose reduces Cur activity. For example, periplasmic fructose binds the sensor protein, BT1754
122 ($\text{Sensor}^{\text{PUL22}}$), which is embedded in the inner membrane. Fructose binding to the $\text{sensor}^{\text{PUL22}}$
123 directly controls the expression of PUL genes responsible for fructose transport via BT1763
124 ($\text{SusC}^{\text{PUL22}}$) and putative phosphorylation by BT1757 ($\text{Frk}^{\text{PUL22}}$) (Extended Data Fig. 2a)[14].
125 Consistent with these studies, a *wild-type Bt* strain harboring P-*PUL22* exhibited increased
126 bioluminescence during growth in PMOG containing 0.2% fructose (Extended Data Fig. 3a) and
127 the addition of fructose increased $susC^{PUL22}$ transcripts 607-fold (Extended Data Fig. 3b). In
128 contrast, a $sensor^{PUL22}$-deficient strain ($\Delta sensor^{PUL22}$) produced no bioluminescence increases
129 when harboring P-*PUL22* (Extended Data Fig. 3a) and $susC^{PUL22}$ transcript amounts did not

130 significantly increase (Extended Data Fig. 3b), indicating that the Sensor^{PUL22} is required to
131 transcribe genes necessary for fructose utilization, in agreement with previous findings[14,24].
132 The Sensor^{PUL22} is also required for fructose-dependent Cur inhibition because
133 *Δsensor^{PUL22}* harboring P-*fusA2* produced similar bioluminescence during growth in PMOG alone
134 or in combination with 0.5% fructose (Fig. 2a). Conversely, bioluminescence from *Δsensor^{PUL22}*
135 was reduced when grown in a mixture of PMOG and glucose (Fig. 2a), similar to *wild-type Bt*
136 (Extended Data Fig. 1e). Furthermore, fructose decreased the abundance of *fusA2* and *chb^{PUL80}*
137 transcripts 181- and 747-fold, respectively, in the *wild-type* strain as previously reported[10], but had
138 no effect in the *Δsensor^{PUL22}* mutant (Fig. 2b & Extended Data Fig. 3c). In contrast, glucose
139 addition to PMOG-grown *Δsensor^{PUL22}* reduced *fusA2* and *chb^{PUL80}* transcripts 809-fold and 1,784-
140 fold, respectively, similar to the 908-fold and 2,058-fold reductions exhibited by *wild-type Bt* under
141 identical conditions (Fig. 2b & Extended Data Fig. 3c). Therefore, the Sensor^{PUL22} is required for
142 Cur inhibition by fructose but not glucose.
143 The PUL22 regulon includes *frk^{PUL22}*, which is putatively responsible for the
144 phosphorylation of fructose as it enters the cytoplasm[25]. Accordingly, *frk^{PUL22}* transcripts increased
145 33-fold in a *sensor^{PUL22}*-dependent manner following the introduction of fructose (Fig. 2c), Frk^{PUL22}
146 protein possessed *in vitro* fructokinase activity (Fig. 2d), and a *frk^{PUL22}*-deficient strain (*Δfrk^{PUL22}*)
147 was unable to grow on fructose (Fig. 2e), indicating that this enzyme is likely the sole *Bt*
148 fructokinase. In contrast, *Δfrk^{PUL22}* did not exhibit a growth defect in glucose (Extended Data Fig.
149 3d) or PMOG (Extended Data Fig. 3e). Fructose phosphorylation is required for entry into central
150 metabolism, but not necessary for Sensor^{PUL22}-directed transcription, because *Δfrk^{PUL22}* harboring
151 P-*PUL22* exhibited increased bioluminescence (Extended Data Fig. 3a) and *susC^{PUL22}* transcript
152 amounts increased 210-fold in *Δfrk^{PUL22}* following the introduction of fructose (Extended Data Fig.
153 3b). Conversely, *susC^{PUL22}* transcript amounts did not increase in *Δsensor^{PUL22}* (Extended Data
154 Fig. 3b). Frk^{PUL22} is necessary for fructose-dependent Cur inhibition because *Δfrk^{PUL22}* harboring
155 P-*fusA2* produced similar bioluminescence during growth in PMOG or a combination of PMOG
156 and fructose but exhibited reduced bioluminescence during growth in PMOG and glucose (Fig.
157 2f), similar to *wild-type Bt* (Extended Data Fig. 1d) and *Δsensor^{PUL22}* (Fig. 2a). Thus, fructose
158 specifically decreases Cur activity via this compartmentalized signaling machinery by increasing
159 fructokinase transcription, suggesting that sugar phosphorylation is necessary to reduce Cur
160 activity.
161 We predicted that glucose phosphorylation mediates Cur inhibition by a distinct
162 mechanism, likely involving a hexokinase, because glucose addition reduced Cur activity

163 independent of Frk^{PUL22} (Fig. 2b and Fig. 2f). BT2493 (Glk) exhibits 92% identity to RokA from
164 *Bacteroides fragilis* (*Bf*), which is necessary for *Bf* growth on glucose[27]. We determined that Glk
165 exhibits glucokinase activity *in vitro* (Extended Data Fig. 4a) and the growth of a *glk*-deficient
166 strain (*Δglk*) was severely impaired on glucose as the sole carbon source but grew similarly to
167 *wild-type Bt* in media containing fructose or PMOG (Extended Data Fig. 4b). Accordingly, *Δglk*
168 harboring P-*fusA2* exhibited similar bioluminescence during growth in media containing PMOG
169 or equal amounts of PMOG and glucose (Fig. 2g). Neither *fusA2* nor *chb*^{PUL80} transcripts
170 decreased following the addition of 0.2% glucose to *Δglk* growing on PMOG (Fig. 2h); however,
171 fructose-dependent silencing resembled *wild-type Bt* (Fig. 2b), indicating that Glk is necessary for
172 glucose, but not fructose, to inhibit Cur activity. Therefore, glucose and fructose require distinct
173 ATP-dependent hexokinases for their utilization and inhibition of Cur activity.
174
175 ***Bt* possesses both ATP- and PPi-dependent glycolytic pathways.**
176 In glycolysis, phosphoglucoisomerase (Pgi) converts glucose-6-phosphate (G6P) into
177 fructose-6-phosphate (F6P), which is subsequently phosphorylated into FBP (Fig. 3a). Because
178 FBP synthesis is the primary regulatory step in glycolysis and *wild-type Bt* cells exhibit reduced
179 FBP amounts[28] with corresponding increases in Cur activity during carbon limitation[10,12], we
180 hypothesized that glucose and fructose reduce Cur activity via this glycolytic step. To test this, we
181 first examined the biochemical activities of 3 putative *Bt* phosphofructokinase (Pfk) enzymes:
182 BT2062 (PfkA), BT1102 (PfkB), and BT3356 (PfkC), whose amino acid sequences share greater
183 than 39% identity with *Ec* PfkA (Extended Data Fig. 5a). We determined that PfkA and PfkB, but
184 not PfkC, are *bona fide* ATP-dependent Pfks, because expression of each in a *pfk*-deficient *Ec*
185 strain[29] restored growth on glucose (Extended Data Fig. 5b) when expressed in an inducer-
186 dependent manner (Extended Data Fig. 5c). Moreover, purified recombinant PfkA and PfkB
187 proteins exhibited activity *in vitro*, whereas PfkC did not (Fig. 3b). Therefore, like *Ec, Bt* encodes
188 two Pfk enzymes that convert F6P into FBP using ATP (Fig. 3a).
189 *Bacteroides* species also encode a putative fructose-6-phosphate 1-phosphotransferase,
190 BT0307 (Pfp), which synthesizes FBP independent of ATP by utilizing pyrophosphate (PPi) as a
191 phosphoryl donor[30]. BT0307 exhibited PPi-dependent FBP synthesis *in vitro*, whereas PfkA and
192 PfkB did not (Fig. 3c). *Bt* expresses *pfkA*, *pfkB*, and *pfp* simultaneously during growth in PMOG
193 and the addition of glucose or fructose decreased *pfkB* and increased *pfp* 2-fold, respectively, but
194 had no effect on *pfkA* transcript amounts (Extended Data Fig. 5d). These results suggest that both
195 ATP- and PPi-dependent FBP synthesis occur simultaneously in the cell; however, PfkA activity
196 was potently inhibited by PPi *in vitro* (Fig. 3d), suggesting its activity is governed by intracellular

197 PPi amounts. Furthermore, PMOG grown *wild-type Bt* exhibited 2.5-fold higher PPi amounts than
198 in fructose-containing media (Fig. 3e), suggesting that fructose utilization permits ATP-dependent
199 FBP synthesis by reducing PPi levels below inhibitory concentrations. Thus, in contrast to other
200 enteric bacteria, *Bt* employs divergent FBP biosynthetic pathways.
201
202 **ATP-dependent FBP synthesis controls Cur activity.**
203 To investigate the role of FBP synthesis in Cur inhibition, we constructed strains lacking
204 *pfkA* (*ΔpfkA*), *pfkB* (*ΔpfkB*), or both *pfkA* and *pfkB* genes (*ΔpfkAB*). *ΔpfkA and ΔpfkB* grew similarly
205 to *wild-type Bt* in fructose or PMOG as sole carbon sources (Fig. 4a, Extended Data Fig. 6a),
206 whereas *ΔpfkA* had slightly increased growth rates and maxima in glucose (Extended Data Fig.
207 6b, c). Unexpectedly, *ΔpfkAB* grew similarly to *wild-type Bt* on fructose (Fig. 4a), glucose, or
208 PMOG (Extended Data Fig. 6a, b, c), implying that ATP-dependent FBP synthesis is dispensable
209 for *in vitro* growth. Cell extracts prepared from *ΔpfkA* or *ΔpfkAB* exhibited no Pfk activity, indicating
210 that ATP-dependent FBP synthesis was entirely absent in these strains (Fig. 4b). In contrast,
211 extracts prepared from *wild-type* and *ΔpfkA* produced indistinguishable PPi-dependent FBP
212 synthesis *in vitro* at rates 11.2- and 38.5-fold greater than ATP-dependent reactions, respectively
213 (Fig. 4b). Conversely, we were unable to generate a strain lacking the *BT0307* open-reading
214 frame, suggesting *pfp* is necessary for growth (Extended Data Fig. 6d), which agrees with
215 transposon-based examinations of essential genes in *Bt*[31,32]. Therefore, PPi-dependent FBP
216 synthesis provides sufficient metabolic flux, thereby rendering ATP-dependent FBP synthesis
217 dispensable for growth.
218 To determine how Pfk enzymes support glycolysis, we measured steady-state metabolite
219 abundances in *wild-type*, *ΔpfkA, ΔpfkB,* and *ΔpfkAB Bt* strains. Accordingly, *ΔpfkA* and *ΔpfkAB*
220 exhibited respective 2.9- and 2.7-fold lower steady-state FBP amounts in *Bt* grown on glucose
221 and fructose, respectively, whereas *ΔpfkB* showed no significant changes in either condition (Fig.
222 4c & Extended Data Fig. 7a) indicating that PfkA is the dominant ATP-dependent FBP biosynthetic
223 enzyme in *Bt*. Downstream glycolytic metabolites, such as dihydroxyacetone phosphate (DHAP),
224 also exhibited corresponding reductions in *ΔpfkA* but not *ΔpfkB* grown in either glucose or fructose
225 (Fig. 4c & Extended Data Fig. 7b). Conversely, PEP and pyruvate amounts were similar across
226 all strains and conditions (Fig. 4c & Extended Data Fig. 7c, d), suggesting these metabolites are
227 maintained by processes independent of PfkA and PfkB. Additionally, *ΔpfkAB* resembled *ΔpfkA*
228 across all metabolites and conditions (Fig. 4c & Extended Data Fig. 7a-d). Finally, ATP-dependent
229 FBP synthesis is necessary for maintaining steady-state nucleotide triphosphates (NTP) and

230 reducing equivalents because ATP and NADH amounts were also reduced in *ΔpfkA* and *ΔpfkAB*
231 (Fig. 4c).
232 To determine if ATP-dependent FBP synthesis contributes to Cur inhibition, we measured
233 bioluminescence in isogenic *wild-type*, *ΔpfkA*, *ΔpfkB*, and *ΔpfkAB* harboring P-*fusA2*. Strikingly,
234 *ΔpfkA* exhibited a 9.2-fold increase in bioluminescence by 12 hours during growth in equal
235 amounts of fructose and PMOG (Fig. 4d) and increased 10.5-fold by the same time point in
236 glucose and PMOG (Extended Data Fig. 8a). Bioluminescence increased further in *ΔpfkAB* over
237 *ΔpfkA,* however, *ΔpfkB* exhibited bioluminescence comparable to *wild-type Bt* harboring an
238 identical reporter plasmid during growth on either mixture (Fig. 4d & Extended Data Fig. 8a).
239 Similarly, *ΔpfkA* and *ΔpfkAB* produced greater bioluminescence than *wild-type* during growth on
240 glucose, fructose, and PMOG as sole carbon sources (Extended Data Fig. 8b, c, d), suggesting
241 that disabling ATP-dependent FBP synthesis increases Cur activity.
242 Consistent with observed bioluminescence increases, *pfkA*, but not *pfkB*, is required for
243 Cur inhibition by glucose and fructose because the *cur*-dependent transcripts *fusA2*, chb^{PUL80}, and
244 *fucI* increased 9.1-, 37.2-, and 3.7-fold respectively in *ΔpfkA* when grown on fructose as the sole
245 carbon source, whereas *ΔpfkB* exhibited transcript amounts indistinguishable from *wild-type* (Fig.
246 4e). Similarly, *ΔpfkA* exhibited respective 2.7-, 6-, and 1.7-fold increased *fusA2* (Fig. 4f), chb^{PUL80}
247 (Extended Data Fig. 8e), and *fucI* (Extended Data Fig. 8f) transcript amounts during growth in
248 glucose that were abolished when the *pfkA* gene was supplied *in trans* (Fig. 4f, Extended Data
249 Fig. 8e, f). The amounts of all three transcripts were indistinguishable between *Δcur* and *ΔpfkA*
250 *Δcur*; but increased in *ΔpfkA Δcur* complemented *in trans* with *cur* but not *pfkA* (Fig. 4f, Extended
251 Data Fig. 8e, f).
252 To explore the possibility of glycolytic intermediates directly impacting Cur's ability to bind
253 its regulated promoters, we performed electromobility shift assays (EMSA) with purified Cur
254 protein and the *wild-type fusA2* promoter or a *Δ22*bp control probe. Increasing amounts of Cur
255 protein shifted the *wild-type fusA2* probe in a dose-dependent manner, with migrations reflecting
256 putative di-, tetra-, and oligo-meric interactions. Conversely, increasing Cur amounts did not alter
257 the migration of the *Δ22*bp probe (Extended Data Fig. 9a-b), indicating that shifting observed with
258 the *wild-type* probe was specific. Glycolytic intermediates that were differentially abundant in
259 *ΔpfkA* are likely indirectly responsible for altering Cur activity because *fusA2* probe shifting was
260 unaltered when F6P, FBP, DHAP, and PEP were included in the assay (Extended Data Fig. 9c).
261 Co-incubation with *Bt* cell lysate fractions also did not change probe migration, suggesting that

262 ligand-dependent probe binding may require different concentrations, additional co-factors, or
263 distinct *in vitro* conditions (Extended Data Fig. 9d).
264
265 **ATP-dependent FBP synthesis regulates Cur *in vivo*.**
266 We hypothesized that PfkA may play a role in intra-intestinal *Bt* fitness because *ΔpfkA*
267 exhibited increased *cur*-dependent products in the presence of simple sugars. Therefore, we
268 inoculated germ-free mice with equal amounts of *wild-type* and *ΔpfkA* and followed their
269 abundance in fecal contents over time. *pfkA* confers a fitness advantage *in vivo* because the
270 relative abundance of *ΔpfkA* decreased 135-fold after 2 weeks (Fig. 5a). This suggests that the
271 demands of intra-intestinal life require ATP-dependent FBP production even though this process
272 reduces growth rates and maxima *in vitro* (Fig. 4a & Extended Data Fig. 6b, c). We also examined
273 the relative abundances of *Δcur* and *ΔpfkA Δcur* following co-introduction into germ-free mice.
274 Strikingly, both strains were present at nearly indistinguishable abundances across two weeks,
275 suggesting that the sole purpose of *pfkA* is to regulate Cur in the mammalian intestine (Fig. 5b).
276 Because PfkA is required for reducing *cur*-dependent products (Fig. 4f and Extended Data
277 Fig. 8e, f), we reasoned that a high sugar diet, primarily comprised of glucose and sucrose, would
278 ameliorate the *ΔpfkA* fitness defect by inhibiting Cur activity in *wild-type Bt*. Accordingly, *ΔpfkA*
279 abundance was reduced only 1.4-fold compared to *wild-type Bt* after 2 weeks in mice provided a
280 sugar-rich chow (Fig. 5a). This indicates that dietary sugar inhibits Cur activity *in vivo* and reduces
281 the *wild-type* strain's advantage over *ΔpfkA*. Finally, sugar-dependent effects on Cur activity are
282 responsible for decreased *Bt* fitness because the abundances of *Δcur* and *ΔpfkA Δcur* were
283 indistinguishable following introduction into germ-free mice fed a sugar-rich diet (Fig. 5b). Taken
284 together, our data demonstrates that ATP-dependent FBP synthesis benefits *Bt* by regulating Cur
285 activity in the mammalian gut and that PfkA activity is required for dietary sugars to inhibit Cur.
286
287 **PfkA regulates Cur activity across human intestinal *Bacteroides* species.**
288 Along with *Bt*, human *Bacteroides* isolates *Bf*, *Bacteroides ovatus*, and *Phocaeicola*
289 *vulgatus* employ Cur to regulate their corresponding *fusA2* orthologs and *Bf* exhibits identical
290 transcript silencing in response to glucose or fructose addition during growth in PMOG[10]. Each
291 species also encodes *pfkA* orthologs (*BF9343_3444*, *BACOVA_00639*, and *BVU_1935*,
292 respectively) and *pfp* orthologs (*BF9343_2852*, *BACOVA_01648*, and *BVU_2286*, respectively)
293 suggesting that ATP-dependent FBP synthesis could govern Cur activity across *Bacteroides*
294 species. We introduced P-*Bf-fusA2 (*p*Bolux* containing the 300 bp region preceding
295 *BF9343_3536)* into *wild-type Bf* and isogenic strains lacking the *pfkA*-ortholog, *BF9343_3444*

296 (*ΔBf-pfkA*) or *cur*-ortholog, *BF9343_0915* (*ΔBf-cur*). A *wild-type* strain harboring P-*Bf-fusA2*
297 exhibited a 12.3-fold increase in bioluminescence compared to a strain harboring a promoter-less
298 p*Bolux* during growth in PMOG (Extended Data Fig. 10a), displaying trends similar to *wild-type*
299 *Bt* harboring P-*fusA2* (Fig. 1d). In contrast, an identical strain exhibited 2.3-fold increased
300 bioluminescence compared to the promoter-less control strain during growth in either glucose
301 (Extended Data Fig. 10b) or fructose (Extended Data Fig. 10c) as the sole carbon source. The
302 addition of glucose (Fig. 6a) or fructose (Fig. 6b) to PMOG reduced bioluminescence from *wild-*
303 *type* harboring P-*Bf-fusA2,* whereas *ΔBf-pfkA* displayed increased bioluminescence under all
304 conditions (Fig. 6a, b & Extended Data Fig. 10a, b, c). As expected, cell extracts from *ΔpfkA*
305 exhibited no ATP-dependent FBP synthesis *in vitro* compared to *wild-type* (Fig. 6c), collectively
306 indicating that this process inhibits Cur activity in *Bf*. Consistent with this notion, bioluminescence
307 from a *Bf* strain lacking both *pfkA* and *cur* (*ΔBf-pfkA ΔBf-cur*) was indistinguishable from *ΔBf-cur*,
308 which were lower than isogenic strains harboring the promoter-less p*Bolux* plasmid (Fig. 6a, b,
309 and Extended Data Fig. 10a, b, c). Therefore, Cur inhibition by ATP-dependent FBP production
310 during growth in dietary sugars is conserved among human *Bacteroides* species.
311
312
313 **Discussion**
314 Our work reveals a pathway in human intestinal *Bacteroides* species required for glucose
315 and fructose to inhibit Cur. We determined that phosphorylation of either monosaccharide requires
316 ATP-dependent sugar kinases necessary for growth, a strategy distinct from traditional PTS that
317 utilizes PEP to phosphorylate sugars upon transport (Fig. 2). Furthermore, we show that *Bt*
318 possesses both ATP- and PPi-dependent enzymes, Pfk and Pfp respectively, which form a
319 hierarchical paradigm to regulate FBP synthesis (Fig. 3) and control Cur activity in response to
320 nutrient availability. We demonstrate that eliminating Pfk alleviates sugar-dependent Cur inhibition
321 without reducing growth (Fig. 4); however, *pfkA* is necessary to control Cur during intestinal
322 colonization (Fig. 5). Furthermore, ATP-dependent FBP synthesis inhibits Cur *in vivo* because the
323 competitive defect exhibited by *ΔpfkA* (Fig. 5b) is abolished when simple sugars are abundant in
324 the host diet. Finally, we established that these processes are conserved in *Bf* and are likely
325 shared among the *Bacteroides* (Fig. 6).
326 Collectively, these data reveal mechanisms that *Bacteroides* species employ to navigate
327 the diverse buffet of intestinal glycans and dietary sugars present in the distal gut. Our findings
328 indicate that Cur activity is tuned based on the type and amount of sugars accessible to
329 *Bacteroides* (Fig. 1d, Extended Data Fig. 1f, g). Furthermore, Cur regulation is likely important to

330 prioritize the metabolism of preferred sugars to compete with other gut bacteria for a limited supply
331 of nutrients. Our findings explain how glucose and fructose consumption hinder *Bacteroides*
332 intestinal fitness by exerting CCR-like effects on Cur activity via two hierarchical FBP biosynthetic
333 pathways. Remarkably, PPi-dependent FBP synthesis occurs at a nearly 12-fold higher rate than
334 ATP-dependent reactions; yet eliminating ATP-dependent synthesis when glucose or fructose is
335 readily available reduced steady-state FBP levels by more than half (Extended Data Fig. 7a). To
336 explain this phenomenon, we propose that the utilization of these simple sugars reduces PPi
337 levels below an inhibitory threshold, thereby simultaneously diminishing the activity of Pfp and
338 allowing for PfkA activity. Furthermore, the essentiality of *pfp*[33] (Extended Data Fig. 6d) and lack
339 of native pyrophosphorylase[30] imply that *Bacteroides* have evolved to rely on PPi, rather than
340 ATP, as a significant glycolytic energy source to conserve ATP. A similar energy-conservation
341 strategy is employed in *Bt* via the *cur*-dependent gene, *fusA2*, whose product preserves NTP
342 pools by facilitating GTP-independent protein synthesis[23]. A deeper examination into the role of
343 PPi-dependent reactions across gut commensals is necessary to understand how bacteria
344 balance NTP and PPi ratios to govern intestinal colonization.

345 FBP is a ubiquitous metabolite that serves as both a glycolytic intermediate and metabolic
346 regulator of other crucial energy pathways[34]. Because endogenous FBP levels are inversely
347 related to Cur activity[28], but do not directly alter its binding to target promoters (Extended Data
348 Fig. 9c), we hypothesize that FBP regulates other important energy pathways in *Bacteroides.* For
349 example, FBP is required to stimulate glycogen production in the *Bacteroidetes* family member,
350 *Prevotella bryantii*[35]. Intriguingly, *Bt* genes encoding putative glycogen metabolic enzymes are
351 important fitness determinants in the murine intestine[31,32] and are necessary for fitness in *cur*-
352 dependent, but not -independent, substrates[33]. In light of this, we propose that host consumption
353 of abundant glucose and fructose reconfigures central metabolism by stimulating ATP-dependent
354 FBP synthesis and glycogenesis, in turn reducing an unknown Cur activator, and ultimately
355 disrupting products necessary for *Bacteroides* fitness and beneficial host interactions.

356 **Methods**

357 *Bacterial strains and growth conditions*

358 All bacteria were cultured as described previously[10] except for *Δglk* strains, which were cultured
359 on rich and minimal media preparations where glucose was replaced with identical concentrations
360 of fructose. Briefly, *Bacteroides* strains were cultured on brain-heart infusion agar (MilliporeSigma)
361 containing 5% horse blood (Hardy) under anaerobic conditions (85% N_2, 12.5% CO_2, 2.5% H_2).
362 Liquid cultures were inoculated from a single colony into TYG media and incubated under
363 anaerobic conditions. All bacterial strains included the following antibiotics where appropriate: 100
364 µg/mL ampicillin, 200 µg/mL gentamicin, 2 µg/mL tetracycline, or 25 µg/mL erythromycin
365 (MilliporeSigma).

366

367 *Engineering chromosomal deletions*

368 Indicated *Bt* genomic deletions were generated using pEXCHANGE-*tdk* plasmids harboring
369 flanking sequences, amplified using the primers listed in Supplementary Table 2, as previously
370 described[36]. In short, pEXCHANGE constructs were introduced via di-parental mating and
371 chromosomal integration was validated by PCR. Parent strains were counter-selected on solid
372 media containing 200ng/mL 5-fluoro-2-deoxyuridine (DOT Scientific). Indicated *Bf* genomic
373 deletions were generated using pLGB13 plasmids harboring flanking sequences, amplified using
374 the primers listed in Supplementary Table 2, as previously described[10,37]. All strains were validated
375 using linear amplicon sequencing.

376

377 *Bacterial growth assays*

378 Bacterial growth was measured as previously described[10]. Briefly, strains were cultured in
379 anaerobic conditions to stationary phase in TYG and diluted 1:200 into reduced minimal media
380 containing the carbon source of interest in 96- or 384-well clear microplates (Corning). Cell growth
381 was monitored using absorbance at 600 nm taken every 15 minutes using a Tecan Infinite M-plex
382 or Nano.

383

384 *Transcription reporter assays*

385 Bioluminescence from each strain was measured in a Tecan Infinite M Plex for 18 hours following
386 1:200 dilution of stationary phase culture in rich media into freshly prepared minimal media
387 containing the indicated carbon sources in 384-well white microplates with clear bottoms
388 (Corning). Each measurement was adjusted by cell growth using absorbance at 600 nm taken

389 every 15 minutes and normalized to isogenic strains harboring the promoter-less p*Bolux* plasmid
390 as previously described[24].
391
392 *qPCR*
393 Stationary phase cultures were diluted 50-fold into pre-reduced minimal media containing the
394 indicated carbon source and incubated to mid-logarithmic phase (OD_{600} = 0.45 - 0.65). For PMOG
395 grown cultures, glucose or fructose was added to a final concentration of 0.2% and incubated for
396 10- or 60-minutes, respectively, before 1.0 mL of culture was pelleted by centrifugation,
397 immediately placed on dry ice, and stored at -80°C. RNA was isolated using the RNeasy Mini Kit
398 (QIAGEN), quantified by absorbance, and 1 µg was converted to cDNA following addition of the
399 Superscript IV VILO Master Mix with ezDNAse (Invitrogen) per the manufacturer's directions.
400 Transcript abundances were measured as previously described[10] using a QuantStudio5
401 (ThermoFisher) and PowerUp SYBR Green Master Mix (ThermoFisher) with amplicon specific
402 primers listed in Supplementary Table 1. The 16S *rRNA, rrs,* was used as the reference gene for
403 all qPCR experiments.
404
405 *E. coli complementation*
406 Plasmids harboring putative *pfk* genes were introduced into the *pfkAB*-deficient *E. coli* strain as
407 previously described[29]. The resulting strains were cultured in M9 minimal media containing
408 glucose as the sole carbon source supplemented with 100 µM IPTG.
409
410 *Protein expression and purification*
411 Proteins were recombinantly expressed as previously described[10]. Briefly, inserts encoding each
412 enzyme were amplified from *B. thetaiotaomicron* VPI-5482 genomic DNA and cloned into pT7-7-
413 N6H4A linearized with NotI-HF and HindIII-HF using NEBuilder Hi-Fi Master Mix (NEB). The
414 resulting plasmids were transformed into chemically competent BL21 cells and plated on selective
415 media. A single colony was inoculated into Luria Bertani broth (BD) and cultured to mid-logarithmic
416 phase before 500 µM IPTG addition and subsequent incubation for 5 hours at 30°C. Pelleted cells
417 were lysed in Lysis Buffer (50 mM sodium phosphate (pH = 7.4) and 300 mM sodium chloride)
418 and N-terminally hexa-histidine-tagged proteins were recovered following co-incubation with Ni^{2+}-
419 NTA resin (Thermo) and elution with Lysis Buffer containing 250 mM imidazole. Recovered
420 proteins were buffer exchanged in 10 mM Tris (pH = 7.4) containing 10% glycerol using
421 appropriate molecular weight cut-off centrifugal concentrators (MilliporeSigma). Protein
422 concentrations were determined using a BCA protein quantification kit (Thermo).

423

424 *Enzyme assays*

425 Crude lysates and recombinant enzymes were tested by coupling glycolytic reactions with NADH
426 oxidation using an excess of the axillary glycolytic enzymes aldolase (ALD), triose phosphate
427 isomerase (TPI), and glyceraldehyde 3-phosphate dehydrogenase (GDH) (MilliporeSigma). All
428 reactions were performed with 5 µg of enzyme, or 50 µL of lysate, in 100 µL of buffer containing
429 of 50 mM Tris (pH = 7.4), 3 mM $MgCl_2$, and 10 mM NH_4Cl. The degradation of NADH was
430 kinetically measured using absorbance at 340 nm with a Tecan Spark. Changes in absorbance
431 across a five-minute linear slope were converted to moles of NADH consumed using a standard
432 curve and normalized by the amount of enzyme to yield the enzymatic rate (nmol/min/µg protein).
433 Enzyme activities were analyzed using non-linear regression and fit to Michaelis-Menten models
434 using GraphPad Prism. PPi inhibition assays were performed in an identical manner with 5 µg of
435 enzyme, 20 mM substrate, and fit to a dose-response model.

436

437 *Quantification of pyrophosphate*

438 *Wild-type Bt* was subbed 1:50 from rich media to minimal media containing the indicated carbon
439 source and grown to mid-logarithmic phase (OD~0.45 - 0.65). Cells pellets were resuspended in
440 1 mL buffer containing 50 mM Tris (pH = 7.4), 3 mM $MgCl_2$, and 10 mM NH_4Cl and immediately
441 boiled. PPi was quantified in resulting extracts using a high sensitivity detection kit
442 (MilliporeSigma) according to the manufacturer's directions.

443

444 *Electromobility shift assays*

445 DNA fragments containing the *fusA2* promoter region were amplified by PCR using Q5 High
446 Fidelity Master Mix and isolated from an agarose gel using a QIAquick gel extraction kit
447 (QIAGEN). Equal amounts of probe and 2 mg/mL poly-dI/dC (MilliporeSigma) were combined with
448 purified Cur protein in binding buffer (20 mM HEPES (pH = 8.0), 10 mM KCl, 2 mM $MgCl_2$, 0.1
449 mM EDTA, 0.1 mM dithiothreitol (DTT), and 10% glycerol) in the presence or absence of 1 mM
450 metabolite or 1 µL fractionated *Bt* lysate to a final volume of 20 µL. Reactions were incubated for
451 20 minutes at room temperature with 4 µL of 6x Native loading buffer, followed by a second, 12-
452 hour incubation at room temperature. Samples containing recombinant Cur, DNA probes, and
453 metabolites or cell extract fractions were then loaded onto a 4-20% TBE gel (Life Technologies),
454 preconditioned in 0.38% TBE, and electrophoresed for 3 hours at 100V. Gels were stained using
455 SYBR green (Invitrogen) per the manufacturer's directions and imaged using an AI680 (GE).

456

457 *Separation of soluble metabolites by liquid chromatography*
458 *Wild-type Bt* cell pellets were lysed in 100-fold lower volume of phosphate buffered saline
459 (MilliporeSigma) by bead beating for five 40-second intervals in a pre-chilled aluminum block
460 interspersed with 5-minute incubations at 4°C, followed by centrifugation for 5 minutes at
461 18,213x*g*. The supernatant was recovered and fractionated using an Agilent Infinity 1260 fitted
462 with a ZORBAX StableBond C18 Column (Agilent). The injection volume was set to 100 µL and
463 samples were eluted using a linear 20 minute gradient (water:MeOH) with a flow rate of 0.5
464 mL/min. Fractions were dried under air and resuspended in 50 µL of ultrapure water for use in
465 EMSA assays.
466
467 *Metabolomics*
468 *Bt* strains were cultured in minimal media containing 5 mg/mL glucose to mid-logarithmic phase
469 (OD~0.45 - 0.65) where 0.5 ODs were collected by centrifugation for 30 seconds, quickly
470 decanted, and immediately flash frozen in a mixture of ethanol and dry ice. Metabolite
471 abundances were measured using Targeted Quantification Analysis by LC-MRM/MS at Creative
472 Proteomics.
473
474 *In vivo competitive fitness of B. thetaiotaomicron strains*
475 All animal experiments were performed in accordance with protocols approved by Penn State
476 Institutional Animal Care and Use Committee. Germ-free C57/BL6 mice were maintained in
477 flexible plastic gnotobiotic isolators with a 12-hour light/dark cycle and provided a standard,
478 autoclaved mouse chow (LabDiet, 5021) or high-sugar chow (Bioserv, S4944) *ad libitum*[10]. Mice
479 were gavaged with 10^8 CFU of each indicated strains suspended in 200 µL of phosphate-buffered
480 saline. Input (day 0) abundance of each strain was determined by CFU plating. Fecal pellets were
481 collected at the desired times and genomic DNA was extracted as described previously[12]. The
482 abundance of each strain was measured by qPCR, using barcode-specific primers (Supplemental
483 Table 2) as described previously[10].
484
485 *Software and statistics*
486 Data collection and curation was done in Microsoft Excel. All data was plotted in GraphPad Prism,
487 except for the heatmap in Fig. 4, which was generated using ggplot2 in RStudio. Statistical
488 analyses were also calculated in Prism. For all experiments, *n* denotes individual biological
489 replicates across two independent experiments.

Acknowledgements

We thank Jordan Bisanz, Donalee McElrath, Michelle Irish, Jacob Perryman, and Alexandra Sprinkle for assistance with germ-free mouse experiments. Additionally, we thank Andrew Goodman, Whitman Schofield, Andrew Patterson, and Imhoi Koo for insights about metabolite measurements. Finally, we thank Jennifer Lausch and Jessica Gaydos for helpful comments during the preparation of this manuscript. This work was supported, in part, by National Institutes of Health Grants DK132711 and GM147178 to G.E.T. and GM123798 to E.A.G.

497 **References**

498 1 Lee, S. H. *et al.* High Added Sugars Intake among US Adults: Characteristics, Eating
499 Occasions, and Top Sources, 2015-2018. *Nutrients* **15** (2023).
500 https://doi.org/10.3390/nu15020265
501 2 Jang, C. *et al.* The Small Intestine Converts Dietary Fructose into Glucose and
502 Organic Acids. *Cell Metab* **27**, 351-361 e353 (2018).
503 https://doi.org/10.1016/j.cmet.2017.12.016
504 3 Khan, S. *et al.* Dietary simple sugars alter microbial ecology in the gut and promote
505 colitis in mice. *Sci Transl Med* **12** (2020).
506 https://doi.org/10.1126/scitranslmed.aay6218
507 4 Wegorzewska, M. M. *et al.* Diet modulates colonic T cell responses by regulating the
508 expression of a Bacteroides thetaiotaomicron antigen. *Sci Immunol* **4** (2019).
509 https://doi.org/10.1126/sciimmunol.aau9079
510 5 Magasanik, B. Catabolite repression. *Cold Spring Harb Symp Quant Biol* **26**, 249-256
511 (1961). https://doi.org/10.1101/sqb.1961.026.01.031
512 6 Loomis, W. F., Jr. & Magasanik, B. The catabolite repression gene of the lac operon in
513 Escherichia coli. *J Mol Biol* **23**, 487-494 (1967). https://doi.org/10.1016/s0022-
514 2836(67)80120-7
515 7 Bruckner, R. & Titgemeyer, F. Carbon catabolite repression in bacteria: choice of the
516 carbon source and autoregulatory limitation of sugar utilization. *FEMS Microbiol Lett*
517 **209**, 141-148 (2002). https://doi.org/10.1111/j.1574-6968.2002.tb11123.x
518 8 Saier, M. H., Jr., Feucht, B. U. & Hofstadter, L. J. Regulation of carbohydrate uptake
519 and adenylate cyclase activity mediated by the enzymes II of the
520 phosphoenolpyruvate: sugar phosphotransferase system in Escherichia coli. *J Biol*
521 *Chem* **251**, 883-892 (1976).
522 9 Simoni, R. D., Roseman, S. & Saier, M. H., Jr. Sugar transport. Properties of mutant
523 bacteria defective in proteins of the phosphoenolpyruvate: sugar
524 phosphotransferase system. *J Biol Chem* **251**, 6584-6597 (1976).
525 10 Pearce, V. H., Groisman, E. A. & Townsend, G. E., 2nd. Dietary sugars silence the
526 master regulator of carbohydrate utilization in human gut Bacteroides species. *Gut*
527 *Microbes* **15**, 2221484 (2023). https://doi.org/10.1080/19490976.2023.2221484
528 11 Schwalm, N. D., 3rd, Townsend, G. E., 2nd & Groisman, E. A. Multiple Signals
529 Govern Utilization of a Polysaccharide in the Gut Bacterium Bacteroides
530 thetaiotaomicron. *mBio* **7** (2016). https://doi.org/10.1128/mBio.01342-16
531 12 Townsend, G. E., 2nd *et al.* A Master Regulator of Bacteroides thetaiotaomicron Gut
532 Colonization Controls Carbohydrate Utilization and an Alternative Protein Synthesis
533 Factor. *mBio* **11** (2020). https://doi.org/10.1128/mBio.03221-19
534 13 Stulke, J. & Hillen, W. Carbon catabolite repression in bacteria. *Curr Opin Microbiol*
535 **2**, 195-201 (1999). https://doi.org/10.1016/S1369-5274(99)80034-4
536 14 Sonnenburg, E. D. *et al.* Specificity of polysaccharide use in intestinal bacteroides
537 species determines diet-induced microbiota alterations. *Cell* **141**, 1241-1252
538 (2010). https://doi.org/10.1016/j.cell.2010.05.005

15 Raghavan, V., Lowe, E. C., Townsend, G. E., 2nd, Bolam, D. N. & Groisman, E. A. Tuning transcription of nutrient utilization genes to catabolic rate promotes growth in a gut bacterium. *Mol Microbiol* **93**, 1010-1025 (2014). https://doi.org/10.1111/mmi.12714

16 Lowe, E. C., Basle, A., Czjzek, M., Firbank, S. J. & Bolam, D. N. A scissor blade-like closing mechanism implicated in transmembrane signaling in a Bacteroides hybrid two-component system. *Proc Natl Acad Sci U S A* **109**, 7298-7303 (2012). https://doi.org/10.1073/pnas.1200479109

17 Barabote, R. D. & Saier, M. H., Jr. Comparative genomic analyses of the bacterial phosphotransferase system. *Microbiol Mol Biol Rev* **69**, 608-634 (2005). https://doi.org/10.1128/mmbr.69.4.608-634.2005

18 Siegel, L. S., Hylemon, P. B. & Phibbs, P. V., Jr. Cyclic adenosine 3',5'-monophosphate levels and activities of adenylate cyclase and cyclic adenosine 3',5'-monophosphate phosphodiesterase in Pseudomonas and Bacteroides. *J Bacteriol* **129**, 87-96 (1977). https://doi.org/10.1128/jb.129.1.87-96.1977

19 Hylemon, P. B. & Phibbs, P. V., Jr. Evidence against the presence of cyclic AMP and related enzymes in selected strains of Bacteroides fragilis. *Biochem Biophys Res Commun* **60**, 88-95 (1974). https://doi.org/10.1016/0006-291x(74)90176-4

20 Ryan, D. *et al.* An expanded transcriptome atlas for Bacteroides thetaiotaomicron reveals a small RNA that modulates tetracycline sensitivity. *Nat Microbiol* **9**, 1130-1144 (2024). https://doi.org/10.1038/s41564-024-01642-9

21 Townsend, G. E., 2nd *et al.* Dietary sugar silences a colonization factor in a mammalian gut symbiont. *Proc Natl Acad Sci U S A* **116**, 233-238 (2019). https://doi.org/10.1073/pnas.1813780115

22 Bry, L., Falk, P. G., Midtvedt, T. & Gordon, J. I. A model of host-microbial interactions in an open mammalian ecosystem. *Science* **273**, 1380-1383 (1996). https://doi.org/10.1126/science.273.5280.1380

23 Han, W. *et al.* Gut colonization by Bacteroides requires translation by an EF-G paralog lacking GTPase activity. *EMBO J*, e112372 (2022). https://doi.org/10.15252/embj.2022112372

24 Modesto, J. L., Pearce, V. H. & Townsend, G. E., 2nd. Harnessing gut microbes for glycan detection and quantification. *Nat Commun* **14**, 275 (2023). https://doi.org/10.1038/s41467-022-35626-2

25 Prezza, G., Liao, C., Reichardt, S., Beisel, C. L. & Westermann, A. J. CRISPR-based screening of small RNA modulators of bile susceptibility in Bacteroides thetaiotaomicron. *Proc Natl Acad Sci U S A* **121**, e2311323121 (2024). https://doi.org/10.1073/pnas.2311323121

26 Carreon-Rodriguez, O. E., Gosset, G., Escalante, A. & Bolivar, F. Glucose Transport in Escherichia coli: From Basics to Transport Engineering. *Microorganisms* **11** (2023). https://doi.org/10.3390/microorganisms11061588

27 Brigham, C. J. & Malamy, M. H. Characterization of the RokA and HexA broad-substrate-specificity hexokinases from Bacteroides fragilis and their role in hexose and N-acetylglucosamine utilization. *J Bacteriol* **187**, 890-901 (2005). https://doi.org/10.1128/JB.187.3.890-901.2005

583 28 Schofield, W. B., Zimmermann-Kogadeeva, M., Zimmermann, M., Barry, N. A. &
584 Goodman, A. L. The Stringent Response Determines the Ability of a Commensal
585 Bacterium to Survive Starvation and to Persist in the Gut. *Cell Host Microbe* **24**, 120-
586 132 e126 (2018). https://doi.org/10.1016/j.chom.2018.06.002
587 29 Lovingshimer, M. R., Siegele, D. & Reinhart, G. D. Construction of an inducible, pfkA
588 and pfkB deficient strain of Escherichia coli for the expression and purification of
589 phosphofructokinase from bacterial sources. *Protein Expr Purif* **46**, 475-482 (2006).
590 https://doi.org/10.1016/j.pep.2005.09.015
591 30 Kuil, T., Nurminen, C. M. K. & van Maris, A. J. A. Pyrophosphate as allosteric
592 regulator of ATP-phosphofructokinase in Clostridium thermocellum and other
593 bacteria with ATP- and PP(i)-phosphofructokinases. *Arch Biochem Biophys* **743**,
594 109676 (2023). https://doi.org/10.1016/j.abb.2023.109676
595 31 Goodman, A. L. *et al.* Identifying genetic determinants needed to establish a human
596 gut symbiont in its habitat. *Cell Host Microbe* **6**, 279-289 (2009).
597 https://doi.org/10.1016/j.chom.2009.08.003
598 32 Liu, H. *et al.* Functional genetics of human gut commensal Bacteroides
599 thetaiotaomicron reveals metabolic requirements for growth across environments.
600 *Cell Rep* **34**, 108789 (2021). https://doi.org/10.1016/j.celrep.2021.108789
601 33 Price, M. N. *et al.* Mutant phenotypes for thousands of bacterial genes of unknown
602 function. *Nature* **557**, 503-509 (2018). https://doi.org/10.1038/s41586-018-0124-0
603 34 Wang, C. Y. *et al.* Metabolome and proteome analyses reveal transcriptional
604 misregulation in glycolysis of engineered E. coli. *Nat Commun* **12**, 4929 (2021).
605 https://doi.org/10.1038/s41467-021-25142-0
606 35 Lou, J., Dawson, K. A. & Strobel, H. J. Glycogen biosynthesis via UDP-glucose in the
607 ruminal bacterium Prevotella bryantii B1(4). *Appl Environ Microbiol* **63**, 4355-4359
608 (1997). https://doi.org/10.1128/aem.63.11.4355-4359.1997
609 36 Koropatkin, N. M., Martens, E. C., Gordon, J. I. & Smith, T. J. Starch catabolism by a
610 prominent human gut symbiont is directed by the recognition of amylose helices.
611 *Structure* **16**, 1105-1115 (2008). https://doi.org/10.1016/j.str.2008.03.017
612 37 Garcia-Bayona, L. & Comstock, L. E. Streamlined Genetic Manipulation of Diverse
613 Bacteroides and Parabacteroides Isolates from the Human Gut Microbiota. *mBio* **10**
614 (2019). https://doi.org/10.1128/mBio.01762-19

615

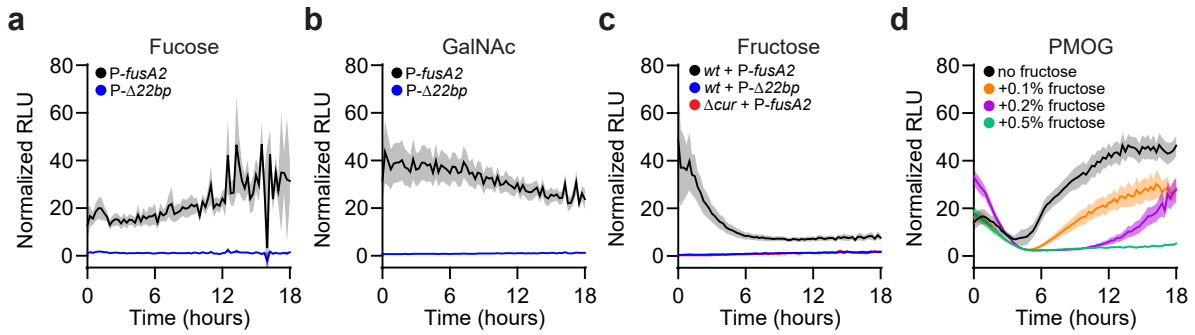

Fig. 1. A bioluminescent transcriptional reporter of Cur activity. a,b, Bioluminescence from a *wild-type Bt* strain harboring P-*fusA2* (black) or P-Δ*22bp* (blue) cultured in media containing **(a)** fucose or **(b)** galNAc as the sole carbon source normalized to measurements collected from isogenic strains harboring a promoter-less p*Bolux* plasmid. **c,** Normalized bioluminescence from a *wild-type* strain harboring P-*fusA2* (black) or P-Δ*22bp* (blue) and a Δ*cur Bt* strain harboring P-*fusA2* (red) cultured in fructose as a sole carbon source. **d,** Normalized bioluminescence from a *wild-type Bt* strain harboring P-*fusA2* cultured in PMOG as the sole carbon source (black) or in combination with 0.1% (orange), 0.2% (purple), or 0.5% (green) fructose. For panels **a-d,** n=8, error is SEM in color matched shading.

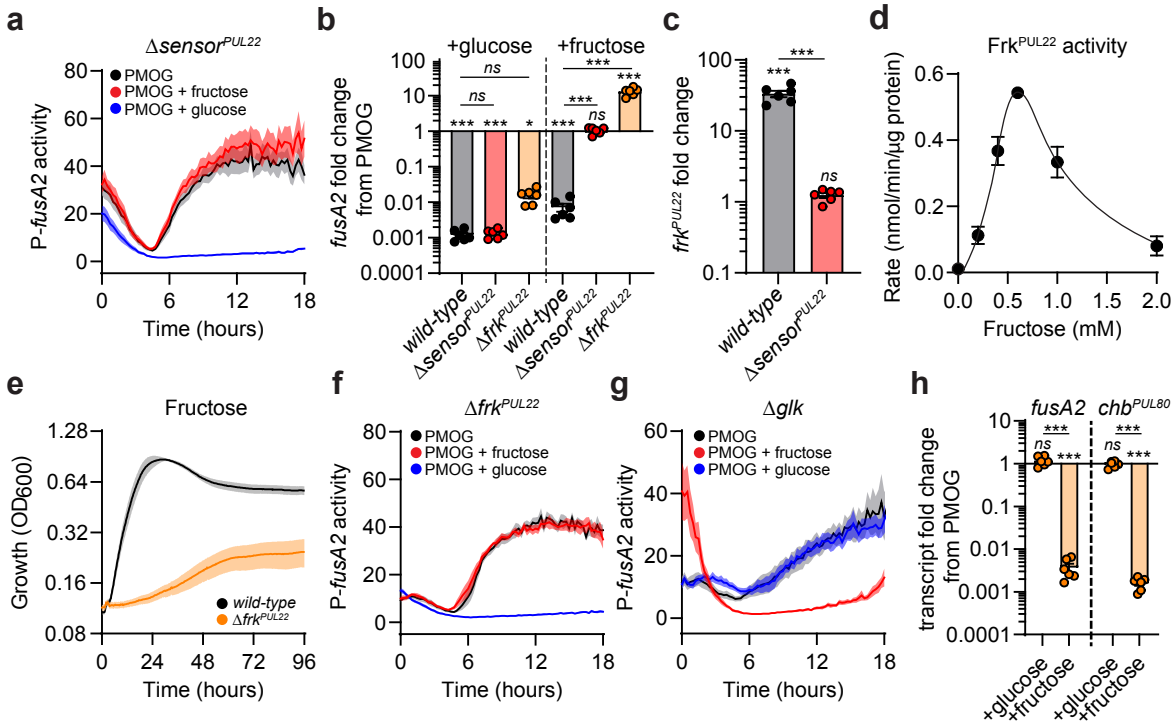

Fig. 2. Fructose and glucose require phosphorylation for Cur inhibition. a, Normalized bioluminescence from Δ*sensor*-^{PUL22} harboring P-*fusA2* cultured in media containing PMOG (black), PMOG and fructose (red), or PMOG and glucose (blue). **b,** Fold change of *fusA2* transcript amounts from *wild-type*, Δ*sensor*^{PUL22}, and Δ*frk*^{PUL22} cultured in media containing PMOG as the sole carbon source 10 minutes following the addition of 0.2% glucose (left) or 60 minutes after 0.2% fructose addition (right). **c,** Fold change of *frk*^{PUL22} transcripts from *wild-type* or Δ*sensor*^{PUL22} 60 minutes following the addition of 0.2% fructose to cells cultured in media containing PMOG. **d,** Fructokinase activity of purified Frk^{PUL22} protein. **e,** Growth of *wild-type* or Δ *frk*^{PUL22} in minimal media containing fructose as the sole carbon source. **f,g,** Normalized bioluminescence from **(f)** Δ*frk*^{PUL22} or **(g)** Δ*glk* harboring P-*fusA2* cultured in media containing PMOG (black) as sole carbon source or equal mixtures of PMOG and fructose (red) or glucose (blue). **h,** Fold change of *fusA2* (left) and *chb*^{PUL80} (right) transcript amounts from Δ*glk* cultured in media containing PMOG as the sole carbon source 10 minutes following 0.2% glucose addition or 60 minutes following fructose addition. For panels **a,e-g,** n=8; error is SEM in color matched shading. For panels **b,c,h,** n=6; error is SEM. For panel **d,** n=4; error is SEM. P-values were calculated by 2-way ANOVA with Fisher's LSD test and * represents values < 0.05, ** < 0.01, *** < 0.001.

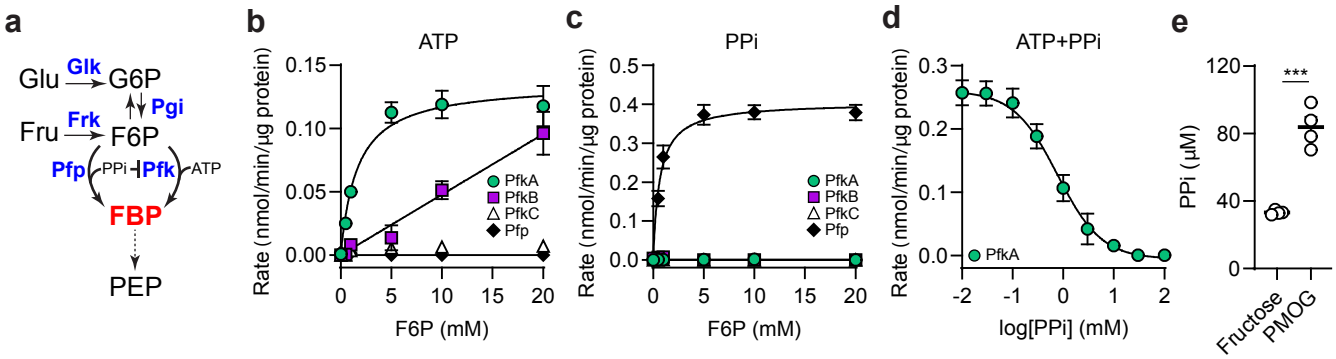

Fig. 3. Distinct enzyme classes synthesize FBP in *Bt*. a, Schematic of the glycolytic pathway in *Bt*. **b,c,** Enzyme kinetics of purified PfkA (green circles), PfkB (purple squares), PfkC (white triangles), or Pfp (black diamonds) in reactions containing either **(b)** ATP or **(c)** PPi as a phosphoryl donor. **d,** PfkA activity in the presence of increasing PPi amounts. **e,** PPi amounts in whole cell lysates of *wild-type* grown in fructose or PMOG as the sole carbon source. For panel **a**, abbreviations are as follows: glucose (Glu), fructose (Fru), glucose-6P (G6P), fructose-6P (F6P), fructose bisphosphate (FBP), phosphoenolpyruvate (PEP), adenosine triphosphate (ATP), pyrophosphate (PPi), phosphofructokinase (Pfk), phosphofructose phosphotransferase (Pfp), phosphoglucose isomerase (Pgi), glucokinase (Glk), fructokinase (Frk). For panels **b-d,** n=4, error is SEM. For panel **e,** n=4, error is SEM; *P*-values were calculated by 1-way ANOVA with Fisher's LSD test and *** represents values < 0.001.

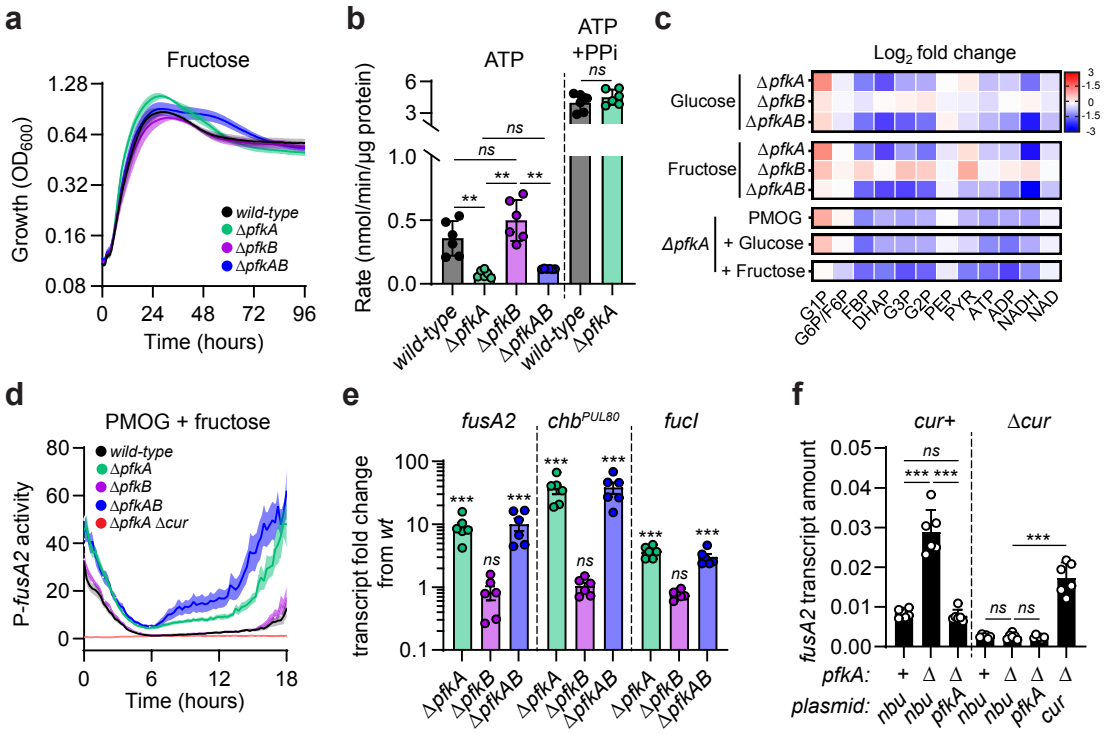

Fig. 4. ATP-dependent FBP production is required for Cur inhibition but dispensable for growth. a, Growth of *wild-type* (black), Δ*pfkA* (green), Δ*pfkB* (purple), or Δ*pfkAB* (blue) in minimal media containing fructose as a sole carbon source. **b,** FBP synthesis measured from whole cell lysates of *wild-type,* Δ*pfkA*, Δ*pfkB*, or Δ*pfkAB*. **c,** Log_2 fold change of steady-state glycolytic intermediates in Δ*pfkA*, Δ*pfkB*, or Δ*pfkAB* in glucose, fructose, PMOG, PMOG with glucose, or PMOG with fructose. **d,** Bioluminescence from *wild-type* (black), Δ*pfkA* (green), Δ*pfkB* (purple), Δ*pfkAB* (blue), or Δ*pfkA* Δ*cur* (red) harboring P-*fusA2* in minimal media containing equal amounts of PMOG and fructose. **e,** Fold change of *fusA2, chb*^{PUL80}*, and fucI* transcript amounts relative to *wild-type* from Δ*pfkA*, Δ*pfkB*, or Δ*pfkAB* cultured in minimal media containing fructose as a sole carbon source. **f,** *fusA2* transcript amounts in *wild-type*, Δ*pfkA*, Δ*cur*, and Δ*pfkA* Δ*cur* harboring empty vector (*nbu*) or complementing plasmids grown in glucose as the sole carbon source. For panel **c,** abbreviations are as follows: glucose-1P (G1P), glucose-6P (G6P), fructose bisphosphate (FBP), dihydroxyacetone-P (DHAP), 3-phosphoglycerate (G3P), 2-phosphoglycerate (G2P), phosphoenolpyruvate (PEP), pyruvate (PYR), adenosine triphosphate (ATP), adenosine diphosphate (ADP), nicotinamide adenine dinucleotide (NAD). For panels **a,d,** n=8; error is SEM in color matched shading. For panel **b,** n=4; error is SEM. For panels **e,f,** n=6; error is SEM. For panels **b,e,f,** *P*-values were calculated by 2-way ANOVA with Fisher's LSD test and * represents values < 0.05, ** < 0.01, *** < 0.001.

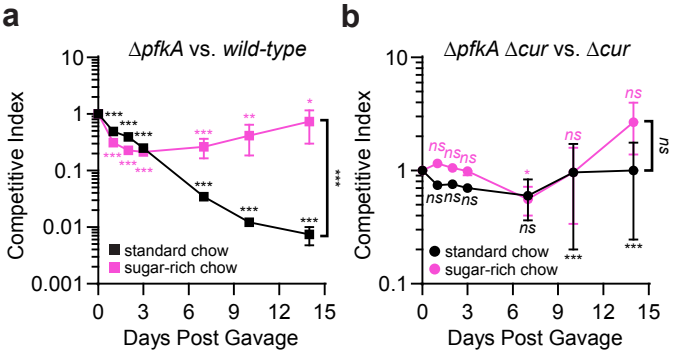

Fig. 5. ATP-dependent FBP production is required for intestinal fitness by controlling Cur. a, Competitive fitness of Δ*pfkA* co-introduced into germ-free mice with equal amounts of *wild-type* and fed a standard polysaccharide rich chow (black squares, n=10) or a sugar-rich chow (pink squares, n = 8). **b,** Competitive fitness of Δ*pfkA* Δ*cur* co-introduced into germ-free mice with equal amounts of Δ*cur* and fed a standard polysaccharide rich chow (black circles, n=10) or a sugar-rich chow (pink circles, n=4). P-values were calculated using 2-way ANOVA with Bonferroni correction and * indicates values < 0.05, ** < 0.01, *** < 0.001.

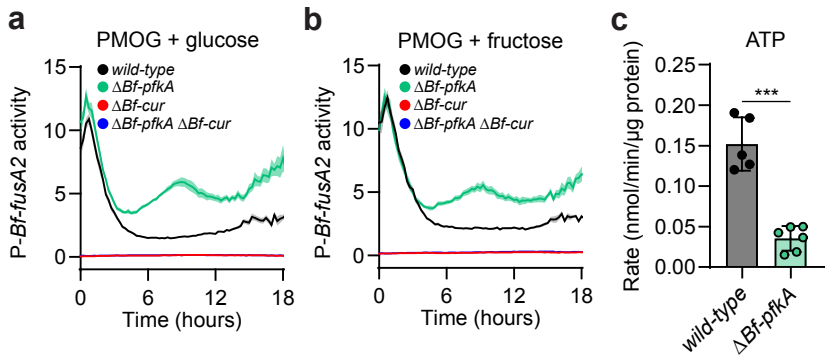

Fig. 6. *Bf-pfkA* is required for glucose- and fructose-mediated Cur inhibition and ATP-dependent FBP synthesis in *B. fragilis*. a,b, Bioluminescence from *wild-type* (black), Δ*Bf-pfkA* (green), Δ*Bf-cur* (red), or Δ*Bf-pfkA* Δ*Bf-cur* (blue) harboring P-*Bf-fusA2* cultured in media containing a mixture of equal amounts of PMOG and **(a)** glucose or **(b)** fructose. **c,** FBP synthetic rates measured from whole cell lysates of *wild-type* or Δ*Bf-pfkA* supplied ATP as a phosphoryl donor. For panels **a,b,** n=8 and error is SEM in color matched shading. For panel **c,** n=5 and error is SEM. P-values were calculated using an unpaired t-test and *** represents values < 0.001.